Diffusion in the presence of scale-free absorbing boundaries

Nir Alfasi[1,2] and Yacov Kantor[1]

[1]*Raymond and Beverly Sackler School of Physics and Astronomy, Tel Aviv University, Tel Aviv 69978, Israel*

[2]*Department of Electrical Engineering, Technion-Israel Institute of Technology, Haifa 32000, Israel*

(Received 4 December 2014; revised manuscript received 10 February 2015; published 22 April 2015)

Scale-free surfaces, such as cones, remain unchanged under a simultaneous expansion of all coordinates by the same factor. Probability density of a particle diffusing near such absorbing surface at large time approaches a simple form that incorporates power-law dependencies on time and distance from a special point, such as apex of the cone, which are characterized by a single exponent η. The same exponent is used to describe the number of spatial conformations of long ideal polymer attached to the special point of a repulsive surface of the same geometry and can be used in calculation of entropic forces between such polymers and surfaces. We use the solution of diffusion equation near such surfaces to find the numerical values of η, as well as to provide some insight into the behavior of ideal polymers near such surfaces.

DOI: 10.1103/PhysRevE.91.042126 PACS number(s): 05.40.−a, 64.60.F−, 82.35.Lr, 02.60.Cb

I. INTRODUCTION

Diffusion in the presence of absorbing boundaries is a well-explored problem [1,2]. It remains an active field of research due to its importance to numerous fields in physics, chemistry, biology, and economy [3–6]. In particular, it is related to the problem of first-passage processes [2,7–9]. In this work, we consider the diffusion of a particle near *scale-free* (SF) surfaces, such as cones of different cross-sections [Figs. 1(a)–1(c)] or a combination of a cone and a plane [Fig. 1(d)]. (Additional examples of SF shapes can be seen in Fig. 1 in Ref. [10].) Such surfaces have no characteristic length scale, i.e., their *shape* is not modified under rescaling by an arbitrary factor λ; i.e., $\vec{r} \to \lambda\vec{r}$. Generally, such scale transformation changes the position of the surface. We will always choose the origin of coordinates as special point on the surfaces, such as apex of the cone, ensuring that the position does not change either. This point will also play an important role in the physical problem: in diffusion problem the particle will be released in the neighborhood of that point, while in the polymer problem one end of the polymer will be held in that vicinity.

The absence of a geometric length scale leads to a rather interesting behavior of the solutions of the diffusion problem, as we explain in Sec. II. In general, the diffusion problem can be related to statistical mechanics of *ideal polymers* in which self-interactions can be neglected [11–13]. In the case of SF surfaces the solutions of diffusion equations can be used to infer the prefactor in force-distance relation characterizing interactions between ideal polymers and the surfaces [10,14,15]. Section III explains the relation between the diffusion and ideal polymer problems, as well as discusses some general features of polymers near surfaces. In this work we employ a simple numerical approach to the problem and demonstrate its usefulness to the quantitative solution of polymer-surface interaction. In Sec. IV we describe our numerical approach, and in Sec. V we use such solutions to gain intuitive insights into the behavior of ideal polymers near repulsive surfaces that have no azimuthal symmetry.

II. DIFFUSION NEAR SCALE-FREE SURFACES

In its most elementary form the diffusion process is described by the probability density $P(\vec{r},\vec{r}_0,t)$ of finding a diffusing particle at a position $\vec{r}$ at time t, if at $t = 0$ it was located at $\vec{r}_0$. Such probability satisfies the diffusion equation

$$\frac{\partial P}{\partial t} = D\nabla^2 P, \tag{1}$$

which must be supplemented by the initial condition $P(\vec{r},\vec{r}_0,t = 0) = \delta(\vec{r} - \vec{r}_0)$, as well as by the boundary conditions. In the presence of *absorbing* boundaries it is required that P vanishes when $\vec{r}$ is on the boundary. Equation (1) corresponds to diffuser in continuous space performing infinitesimal steps. For a random walker on a d-dimensional periodic (e.g., hypercubic) lattice with lattice constant a, with dimensionless time measuring the number of discrete steps, the Laplacian in Eq. (1) is replaced by its discrete version, while the time derivative of P becomes a difference in probabilities at (dimensionless) times $t + 1$ and t. In this case the diffusion constant becomes $D = a^2/2d$. (The theory presented here is valid at arbitrary d, but the numerical examples will focus on simulations performed on a three-dimensional cubic lattice.) In the presence of absorbing boundaries, the survival probability $S(\vec{r}_0,t) = \int P(\vec{r},\vec{r}_0,t)d^d r$ of a particle that at time $t = 0$ was at point $\vec{r}_0$ decays with time. The function S also satisfies [16] diffusion Eq. (1) with spatial derivatives taken with respect to variable $\vec{r}_0$, but its initial condition is $S(\vec{r}_0,t = 0) = 1$ inside the permitted volume while vanishing (at any t) on the absorbing boundary.

The trace of a particle diffusing on a lattice for time $t = N$ can be viewed as a configuration of an ideal polymeric chain with $N + 1$ monomers [11–13]. In the absence of confining surfaces the number of different configurations starting at a specific lattice site $\vec{r}_0$ is $\mathcal{N}(\vec{r}_0,N) = z^N$, where z is the coordination number of a lattice. If *repulsive* boundaries are present, the configurations that cross the boundary must be excluded. This is accounted for by considering a random walk (RW) problem with *absorbing* boundary conditions, and $\mathcal{N}(\vec{r}_0,N) = z^N S(\vec{r}_0,N)$. Thus, solution of the diffusion problem provides a handle on counting the configurations of ideal polymers. The latter determines the free energy of the polymers and can be used to find forces between the polymers and confining surfaces [14,15].

Solution of diffusion Eq. (1) in a *finite* space surrounded by absorbing surfaces can be presented in the form [17]

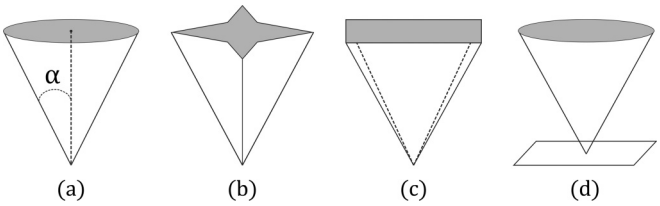

FIG. 1. Examples of scale-free surfaces: cones with (a) circular, (b) star-shaped, and (c) square cross-sections, and (d) a circular cone touching a plane. All shapes are infinite, with gray surfaces indicating truncation for graphic purposes.

$P(\vec{r},\vec{r}_0,t) = \sum_i A_i \Phi_i(\vec{r}) e^{-t/\tau_i}$, where Φ_i and $1/\tau_i$ are the eigenfunctions and eigenvalues of the equation $\nabla^2 \Phi_i = -\Phi_i/\tau_i$, while the prefactors A_i depend on the initial position $\vec{r}_0$ of the particle. Similarly, the survival probability $S(\vec{r}_0,t) = \sum_i B_i \Phi_i(\vec{r}_0) e^{-t/\tau_i}$ [17]. For long times the behavior of both functions will be dominated by the smallest eigenvalue $1/\tau_1$, i.e., $P \propto \Phi_1(\vec{r}) e^{-t/\tau_1}$, and $S \propto \Phi_1(\vec{r}_0) e^{-t/\tau_1}$. Typically, the value of the largest time $\tau_1 \sim \ell^2/D$, where ℓ is the largest linear dimension of the confining volume. If the confining volume is *not finite* the solution never reaches the state of exponential decay. In this work, we consider the diffusion of a particle near SF surfaces. Since both the equation, and the boundary and initial conditions imposed on $S(\vec{r}_0,t)$ are SF, S can only depend on the scaled (dimensionless) variable $\vec{w} = \vec{r}_0/\sqrt{Dt}$. Moreover, for $w \ll 1$ the Eq. (1) reduces to $\nabla^2_{\vec{w}} S = 0$, where the derivatives of the Laplacian are taken with respect to $\vec{w}$. In this limit we expect a simple power law solution [8]

$$S = w^\eta g(\{\theta_i\}) = (r_0/\sqrt{Dt})^\eta g(\{\theta_i\}), \tag{2}$$

where g is a function of $d-1$ angular variables $\{\theta_i\}$ [10], which solves the eigenvalue equation

$$\Delta_{S^{d-1}} g = \eta(2-d-\eta) g, \tag{3}$$

where $\Delta_{S^{d-1}}$ is the spherical Laplacian [18]. Angular variables represent position on a unit sphere and we expect a discrete spectrum of values of $\eta = \eta_i$. We are interested in large t (small w) limit, and therefore choose η to be the smallest eigenvalue of Eq. (3). Since the probability density must be positive, the eigenfunction corresponding to that η is a function that does not change sign [8]. We note that Eqs. (2) and (3), as well as the equations that will be derived from them in Sec. IV, are valid for any SF surfaces and do not require additional symmetries, such as azimuthal symmetry.

III. DIFFUSION AS A POLYMER PROBLEM

Many properties of polymers in free space [11] and near limiting surfaces [19–21] can be deduced from the theory of critical phenomena. In particular, some behaviors are characterized by critical exponents that are independent of microscopic details of the Hamiltonian. Such universality enables usage of simplified models, such as RWs on lattices representing ideal polymers, or self-avoiding walks (SAWs) representing polymers in good solvent [11,22]. On a regular lattice, the number of conformations of a polymer in free space is $\mathcal{N} \propto z^N N^{\gamma-1}$, where z is the lattice coordination number in the case of a RW, and an effective coordination number in the case of SAW. Critical exponent γ is universal [11]. This exponent is related by Fisher's identity [23] to correlation length exponent ν and the exponent η characterizing the anomalous decay of density correlations: $\gamma = (2-\eta)\nu$. Values of the exponents γ, ν, and η differ between RWs and SAWs. In this paper we deal only with *ideal polymers* model for which $\nu = 1/2$ [22].

Presence of scale-invariant boundaries modifies the behavior of polymers. In the expression for the number of configurations $\mathcal{N} \propto z^N N^{\gamma-1}$, the leading *nonuniversal* part z^N remains unchanged! Similarly, there is no change in the correlation length exponent ν [19–21]. However, the exponent γ characterizing the *subleading* N-dependence of $\mathcal{N}$ changes its value. (For flat surfaces it is frequently denoted γ_1 [19], while for wedges with opening angle α it is sometimes denoted $\gamma_2(\alpha)$ [24].) As their free-space counterparts, these exponents do not depend on the microscopic details of the Hamiltonian, but their values *do depend* on the type of the limiting surface. Exponent η describing the behavior of the correlation functions is also affected by the presence of the surface. However, Fisher's relation, which is a consequence of the fact that the total number of states is an integral of the correlation function, remains valid even in those modified circumstances; e.g., for a flat surface $\gamma_1 = (2-\eta_\perp)\nu$, where $\eta_\perp$ describes the power-law dependence of the correlation function in any direction except parallel to the surface [24]. This relation persists also for wedges and cones. In our problem, all the exponents correspond to specific surfaces under consideration and we omit the various subscripts used in the literature. Since we are considering only *ideal polymers*, Fisher's relation for our surface-specific exponents reduces to $\gamma - 1 = -\eta/2$ leading to $\mathcal{N} \propto z^N N^{-\eta/2}$. By comparing this expression with Eq. (2) with $t = N$ we see that this is the same exponent η as was defined in the diffusion problem for the same type of surface.

Our goal is to establish numerical value of the exponent η in a variety of geometries for ideal polymers. In simple geometries [such as circular cones (in $d = 3$) or wedges (in $d = 2$)] this exponent is known analytically [8,10,14,15]. (In some cases, η is known even for polymers in good solvents [22], where it is found by studying numerically SAWs in $d = 3$ for flat surfaces [19,20,25] and for circular cones or cone-plane geometries [14,15].)

Polymers can mediate forces between two surfaces. Consider a polymer attached by one end to a special point of one SF surface that is brought close (distance h) from a special point of another SF surface. As an example, we may consider a polymer attached to an apex of a cone that is being brought into the vicinity of a plane. This resembles measurements done by means of an atomic force microscope (AFM) [26,27], where a long molecule is attached to the sharp tip of a probe and the probe is brought into the vicinity of a flat stage. (However, in a typical experimental situation the *other* end of the polymer is also attached to the stage.) The loss of polymer entropy leads to entropic force between the two objects [14,15]:

$$F = \mathcal{A}\frac{k_B T}{h}, \tag{4}$$

where $\mathcal{A}$ is a dimensionless prefactor. This relation is true only for h much smaller than the root-mean-squared end-to-end distance of the polymer. (In the absence of any additional

length scales, this is the only possible dimensionally correct expression for the force.) The change in free energy of the polymer when bringing one object into contact with the second one is due to the change in entropy $S = k_B \ln \mathcal{N}$. Both the initial and final states of the system (but not the intermediate ones) are SF and can be characterized using the exponents η. The difference in the entropy (and free energy) of the two states must be equal to the work performed by the force. Since the leading exponential part of the number of states z^N, which corresponds to the leading *extensive* part of the entropy and free energy, is identical in both SF situations, the difference in the free energies is proportional to the difference of the subleading terms $(\gamma_{\text{initial}} - \gamma_{\text{final}}) \ln N$. Comparison of this relation with the integral of the force in Eq. (4) over the separation h between a microscopic distance a and the maximal interaction distance $\sim aN^{\nu}$ fixes the value of the prefactor [14,15]:

$$\mathcal{A} = \eta_{\text{final}} - \eta_{\text{initial}}. \tag{5}$$

Thus, the force between two surfaces, mediated by the polymer, depends solely on the geometry of the surfaces through the exponents η corresponding to the initial and the final states. Equations (4) and (5) have been derived [14,15] by assuming equilibrium conditions. Long equilibration times of polymers [11] make the equilibrium measurements of force-position relations a difficult task. For *slightly* nonequilibrium energy-dominated experimental situations Crooks fluctuation theorem [28] can be used to recover some equilibrium properties from nonequilibrium experiments [29].

IV. THE METHOD

Since calculation of the force constant has been reduced to finding η in SF geometries, our aim is to consider simple methods for accomplishing this task. For ideal polymers in high symmetry systems, such as three-dimensional problem of a circular cone [Fig. 1(a)], including its particular cases of plane or semiinfinite line, or a circular cone attached to a plane perpendicular to its axis [Fig. 1(d)], it is possible to solve Eq. (3) analytically (see, e.g., Refs. [8,14,15]). (Such solutions can also be obtained in arbitrary d.) However, even in simple figures such as cones with square or star-shaped cross-section, the solution of the eigenvalue equation becomes rather cumbersome. Fortunately, there is another, rather simple numerical approach to the problem described in the following paragraphs.

Consider solving the time-dependent Eq. (1), beginning with the $\delta(\vec{r} - \vec{r}_0)$ initial condition for P and evolving the equation in time. At very short times P will resemble free space solution uninfluenced by the boundaries. If the starting point is at some distance r_0 from an apex of the cone, then at time $t \sim \tau \equiv r_0^2/D$ the influence of the boundaries will be strongly felt, and for $t \gg \tau$ the initial conditions will be forgotten. The solution of the problem will approach [10]

$$P(\vec{r},t) = At^{-\eta-d/2} r^{\eta} \exp\left\{-\frac{r^2}{4Dt}\right\} g(\{\theta_i\}), \tag{6}$$

where only the prefactor A will depend on $\vec{r}_0$. It is possible to verify directly that this expression solves the differential Eq. (1) *exactly*, provided g and η are solutions of Eq. (3). This solution, however, does not satisfy the exact initial conditions

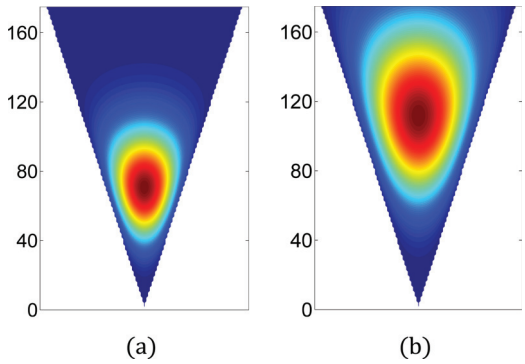

FIG. 2. (Color online) Vertical cross section of $P(\vec{r},t)$ of particle diffusing inside circular cone with apex angle $\alpha = \pi/10$ and absorbing boundaries. At $t = 0$ the particle is located a few lattice constants away from the apex. Probability density is shown at (a) $t_1 = 2000$ and (b) $t_2 = 5000$. The *shape* of the function does not change with time: by expanding (a) by a factor $\sqrt{t_2/t_1}$ it will coincide with (b).

and can be used only for sufficiently long times. In the absence of geometric length scale, the distance r from the apex in Eq. (6) can be only compared with $\sqrt{Dt}$. Thus, the shape of the function does not change over time except for being stretched. Figure 2 depicts the numerical solution for a diffusing particle inside a circular cone with absorbing boundaries calculated on a cubic lattice. The simulation begins with the particle situated on a lattice site close to the apex of the cone and the probability is then evolved by using discrete diffusion equation, i.e., the probability at a particular lattice site (inside the permitted space) at time $t + 1$ is equal to the mean of the probabilities at the neighboring sites at time t. The absorbing boundary conditions are implemented by keeping probability 0 outside the permitted space. Due to the absorption, the total survival probability decreases. The color-coding in this and other pictures depicting the density was chosen to be a linear scale ranging from dark blue (=0) to dark red (=maximum), thus removing the effect of overall decrease of the function. Figures 2(a) and 2(b) depict the probability at two different times. Both functions seem to have the same shape spread over distances much larger than the few lattice constants that the initial position $\vec{r}_0$ was separated from the apex of the cone. This persistence of the shape confirms the claim that the position of the starting point has been "forgotten."

As expected, the integral of Eq. (6) over the space produces $S \propto t^{-\eta/2}$, which can be used to determine the exponent η [30,31]. Numerically, this can be accomplished by simply summing up all the probabilities at several times t and extrapolating the *slope* of the graph (on a logarithmic scale) to large times. The method presented below offers a slightly more convenient alternative into measuring η.

We notice that the exponential term in Eq. (6) is exactly the same as it would be in the absence of boundaries. The absorbing boundaries generate the time-dependent (power law) prefactor, as well as term r^{η}. While the probability density in Eq. (6) is not normalized due to absorbtion, we may calculate the mean-squared distance R^2 of a *surviving* particle from the apex $R^2 = \int r^2 P(\vec{r},t) d^d r / \int P(\vec{r},t) d^d r$. In this ratio of integrals, the prefactors and the angular integrals cancel out,

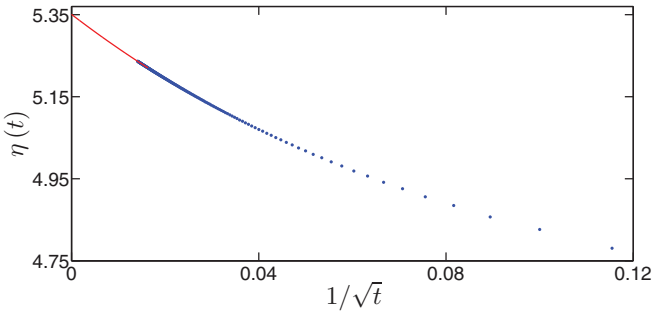

FIG. 3. (Color online) Dependence of the effective exponent $\eta(t)$ on simulation time t up to $t = 5000$ for a cone with star-shaped cross-section [see Fig. 1(b)] with inner apex angle $\alpha = \pi/4$, and the apex angle of the outer point equal $\pi/\sqrt{2}$. The residual t-dependence is evident. By fitting the data by quadratic polynomial in $1/\sqrt{t}$ (solid line) we obtain the extrapolated value $\eta = 5.35$.

and we are left with the ratio of two simple integrals leading to

$$R^2 = 2Dt(\eta + d). \tag{7}$$

Note, that in the absence of boundaries $\eta = 0$, and the above result reduces to the well-known free-space expression $R^2 = 2dDt$. For large time, R^2 coincides with mean-squared traveled distance by the walker, or mean-squared end-to-end distance of an ideal N-step polymer for $N = t$. Since the numerical evolution of the diffusion equation is a very simple task, we can use Eq. (7) to calculate exponent η, by finding the large t limit of $(R^2/2Dt) - d$. Of course, for finite times we expect corrections due to discreteness of the lattice, presence of ragged boundaries on a lattice, and due to the fact that the walker begins its path few lattice constants away from the apex. Each of these problems has a typical length scale of the order of lattice constant a, and their influence will disappear when the dimensionless ratio $a/R \sim 1/\sqrt{t} \ll 1$. Naturally, we expect the t-dependent effective exponent $\eta(t) = \eta + c_1/\sqrt{t} + c_2/t + \cdots$, where the first term is the anticipated actual value of the exponent. Figure 3 depicts the time-dependence of $\eta(t)$ for a cone of star-shaped cross-section measured up to $t = 5000$. Last calculated point is only few percent away from the intercept ("$t \to \infty$") with the vertical axis at $\eta = 5.35$, which was obtained by extrapolating the numerical values using a quadratic polynomial in $1/\sqrt{t}$. Our method requires solution of the diffusion equation, i.e., its numerical complexity does not differ from the calculation relying on the measurement of the power-law dependence of the survival probability mentioned in the previous paragraph. However, we believe that it provides a slightly more convenient alternative.

Exponent η for an ideal polymer attached to a contact point between a plane and a cone perpendicular to that plane, as depicted in Fig. 1(d), can be found analytically [14,15]. In this three-dimensional geometry with azimuthal symmetry the eigenvalue Eq. (3) becomes Legendre equation, and the eigenfunction $g(\theta)$ can be expressed as a linear combination of regular Legendre functions of degree η. The value of η in this cone-plane geometry depends on the apex angle α of the cone and is determined as the (smallest) value

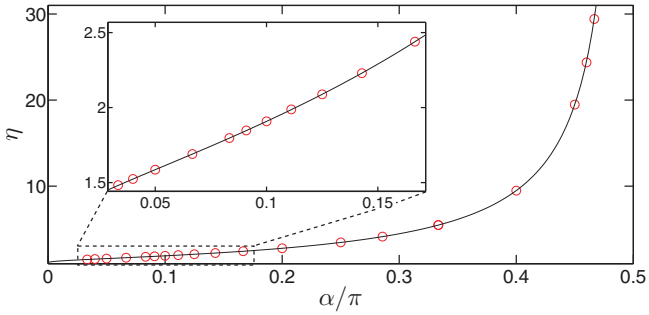

FIG. 4. (Color online) Exponent η as function of apex angle α for cone-plane geometry depicted in Fig. 1(d). Our numerical results (circles) are compared with the known analytical values [15] (solid line).

for which the absorbing boundary condition ($g(\theta = \alpha) = 0$) is satisfied [15]. Figure 4 depicts the results of numerical evaluation of the exponent compared with the known analytical values. Excellent correspondence of the results validates our numerical procedure. As the apex angle increases, the number of polymer configurations trapped between the cone and the plane that it touches decreases as can be seen in the increasing value of η. For $\alpha \to \pi/2$ the exponent η diverges, as expected. As α increases, so does the numerical difficulty to obtain accurate estimate of η, requiring larger times t.

V. EXPONENT η FOR GEOMETRIES WITHOUT AZIMUTHAL SYMMETRY

While analytical values of η could be found for the cone perpendicular to the plane considered in the previous section, tilting the cone axis by angle β with respect to the normal to the plane (see sketch in Fig. 5) breaks the azimuthal symmetry and prevents a simple analytical solution. We therefore find values of η as function of β numerically, for $\alpha = \pi/5$, $\pi/10$, and $\pi/20$, as depicted in Fig. 5. The tilts are, of course, limited by the inequality $\beta \leqslant (\pi/2) - \alpha$. The maximal value of η for any α is achieved for an upright cone, and the values decrease with increasing tilting. For a polymer attached to a planar surface, i.e., in the case of completely absent cone, $\eta = 1$. The cone with $\alpha = \pi/20$ almost reaches that value when it is tilted to the maximal extent. The other two cases also exhibit

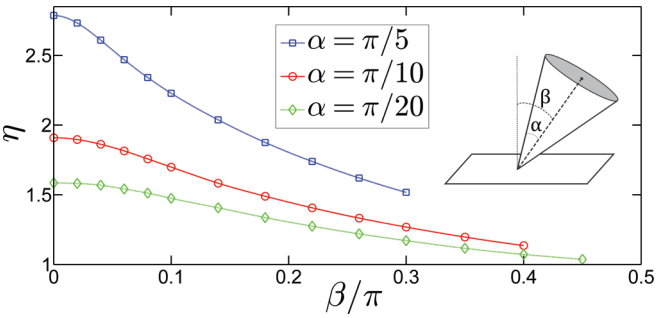

FIG. 5. (Color online) Exponent η as function of tilt angle β for a tilted circular cone touching a plane for three apex angles (top to bottom) $\alpha = \pi/5$ (square), $\alpha = \pi/10$ (circle), and $\alpha = \pi/20$ (diamond). The solid lines interpolate between numerical results.

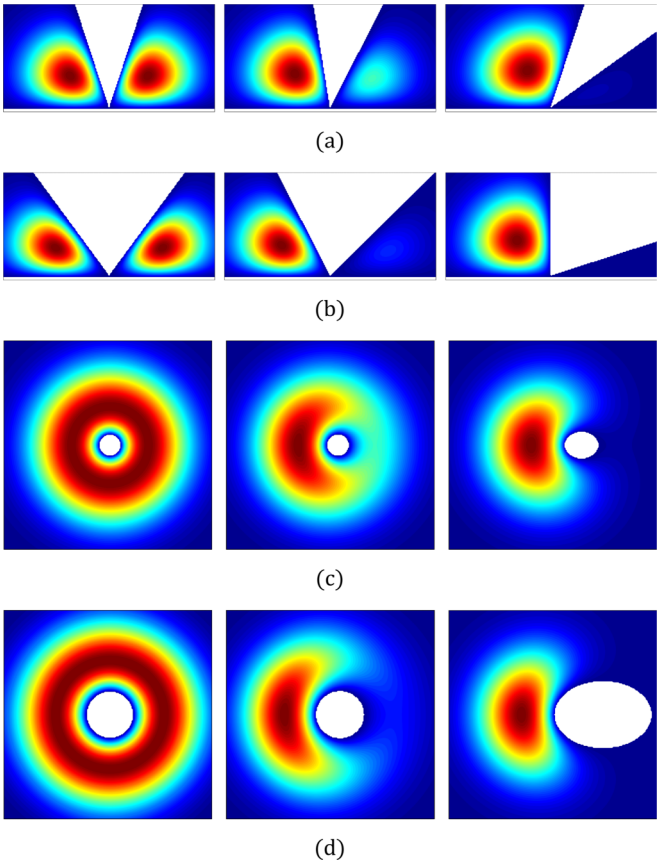

FIG. 6. (Color online) Probability density P for diffusing particle in the vicinity of cone touching a plane. Cross-sections perpendicular to the plane contacted by the cone include the axes of the cones. Two apex angles (a) $\alpha = \pi/10$ and (b) $\pi/5$ are considered. Panels (c) and (d) show cross-sections parallel to the plane contacted by the cone for those apex angles. This section is made at height 30 lattice constants at time $t = 4000$. This is the level where P is close to its maximum value. The left column shows upright cone ($\beta = 0$), while the center and right columns show tilts of $\beta = 0.05\pi$ and 0.15π, respectively.

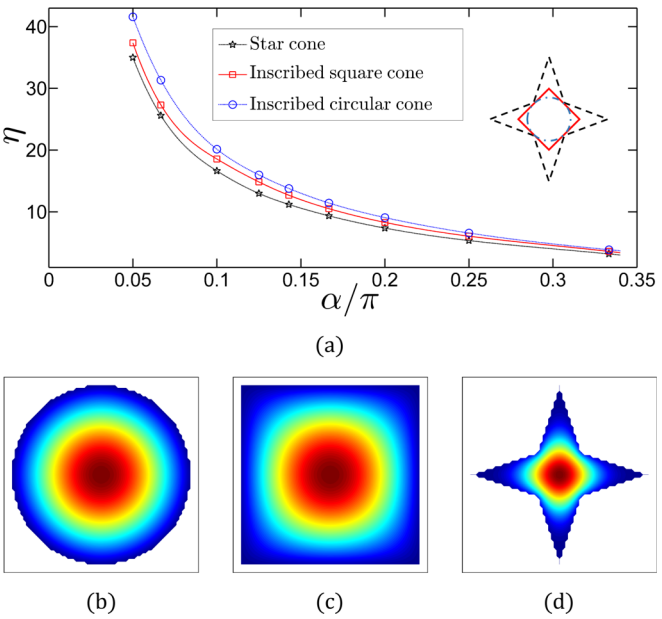

FIG. 7. (Color online) (a) Exponent η as function of apex angle α of a circular cone and for cones of square- and star-shaped cross-section circumscribed around the circular cone as depicted in Figs. 1(a)–1(c), as well as in the embedded sketch. The outer radius of the star-shaped cone is $2^{3/2}$ times larger than its inner radius. Symbols indicate the numerical values, while the continuous lines interpolate between the calculated values. Bottom part of the figure depicts transverse cross-sections of $P(\vec{r},t)$ for inside (b) circular, (c) square-shaped, and (d) star-shaped cones. All sections were performed 100 lattice constants away from the apex for $t = 4000$ and α of a circular cone equal to $\pi/10$.

a significant decrease with increasing β. This means that an upright cone causes the maximal constriction of the space available to the polymer, while the tilt significantly decreases that effect. Figure 6 depicts the cross-sections probability density in planes parallel and perpendicular to the plane that is touched by the cone for two apex angles α. We can clearly see that even for small tilts the polymer "escapes" to the more open part of the space, where its configurations somewhat resemble the behavior of a polymer in half-space in the absence of a cone.

Finally, we consider diffusing particles inside cones with circular, square, and four-point star cross-sections [Figs. 1(a)–1(c)]. Figure 7(a) depicts the dependence of the exponent η for several cross-section shapes as a function of an opening angle, while Figs. 7(b)–7(d) show transverse cross-sections of $P(\vec{r},t)$ for the three different shapes. An interesting feature is seen in Fig. 7(d), where $P(\vec{r},t)$ inside the star-shaped cone resembles that of diffusion inside the square-shaped cone, rotated by 45°. This implies that the surviving(!) diffusing particle is less likely to be found deep inside the star's wings and can be found in the center of the star with much higher probability. This feature is also seen in Fig. 7(a), where the values of ηs are similar, though not identical, in the two geometries.

VI. DISCUSSION

In this paper we examined the long-time solutions of the diffusion equation in the presence of SF-absorbing boundaries and found the probability density function of a diffusing particle. Unlike finite spaces that are characterized by finite absorption times and exponential decay of survival probability, SF-absorbing shapes generate survival functions that decay as power law $t^{-\eta/2}$. The same exponent appears in the spatial part of the probability density of a diffusing particle and can be calculated from the measurement of mean-squared distance traveled by surviving particle. Our results provide information regarding the behavior of ideal polymers. In high space dimension the solid angle describing the cone plays a major role in determining the value of η, while specificities of the shape are not very important [9,31]. Our results with tilted cones, as seen in Fig. 5, or with cones with various cross-sections demonstrate the sensitivity of the values of η on the shape details in $d = 3$ for a fixed solid angle.

In real experiments we are more likely to encounter polymers described by different statistics. In particular, polymers in good solvents are better described by self-avoiding walks [11]. For ideal polymers the simple relation between R^2 and the

exponent η as shown in Eq. (7) was a specific consequence of long-time solution in Eq. (6), which is a product of a power law and a Gaussian with respect to variable r. Polymers in good solvents have a slightly different functional dependence on r, which does not permit a simple identification of η from the probability distribution of their end-point for a single value of N. Nevertheless, the general expression for the force constant in Eqs. (4) and (5) remains valid, while the values of the exponents η maintain similar shape dependencies and are surprisingly *close numerically* to the values of ηs for ideal polymers [14,15,32]. Therefore, our results, besides providing some intuition regarding the polymers in good solvents, also provide reasonable guesses for the numerical values of the exponents in such solvents.

ACKNOWLEDGMENTS

We thank Y. Hammer and M. Kardar for numerous discussions. This work was supported by the Israel Science Foundation Grant No. 186/13.

[1] H. S. Carslaw and J. C. Jaeger, *Conduction of Heat in Solids*, Vol. 2 (Oxford University Press, Oxford, 1959).
[2] S. Redner, *A Guide to First-Passage Processes* (Cambridge University Press, Cambridge, 2001).
[3] G. H. Weiss, *Aspects and Applications of the Random Walk* (North-Holland, Amsterdam, 1994).
[4] H. C. Berg, *Random Walks in Biology* (Princeton University Press, Princeton, NJ, 1993).
[5] M. Kimura, J. Appl. Prob. **1**, 177 (1964).
[6] A. Abraham, F. J. Seyyed, and S. A. Alsakran, Financial Rev. **37**, 469 (2002).
[7] B. D. Hughes, *Random Walks and Random Environments*, Vol. 1 (Oxford University Press, New York, 1995).
[8] E. Ben-Naim and P. L. Krapivsky, J. Phys. A **43**, 495007 (2010).
[9] E. Ben-Naim and P. L. Krapivsky, in *First-Passage Phenomena and Their Applications*, edited by R. Metzler, G. Oshanin, and S. Redner (World Scientific, Singapore, 2014).
[10] Y. Hammer and Y. Kantor, Phys. Rev. E **89**, 022601 (2014).
[11] P. G. de Gennes, *Scaling Concepts in Polymer Physics* (Cornell University Press, Ithaca, NY, 1979).
[12] M. Rubinstein and R. H. Colby, *Polymer Physics* (Oxford University Press, New York, 2003).
[13] M. Doi, *Introduction to Polymer Physics* (Clarendon Press, Oxford, 1996).
[14] M. F. Maghrebi, Y. Kantor, and M. Kardar, Europhys. Lett. **96**, 66002 (2011).
[15] M. F. Maghrebi, Y. Kantor, and M. Kardar, Phys. Rev. E **86**, 061801 (2012).
[16] F. W. Wiegel, *Introduction to Path-Integral Methods in Physics and Polymer Science* (World Scientific, Singapore, 1986).
[17] P. M. Morse and H. Feshbach, *Methods of Theoretical Physics*, Vol. 1 (McGraw-Hill, New York, 1953).
[18] S. Rosenberg, *The Laplacian on a Riemannian Manifold* (Cambridge University Press, Cambridge, 1997).
[19] K. Binder, in *Phase Transitions and Critical Phenomena*, edited by C. Domb and J. L. Lebowitz (Academic Press, London, 1983), Vol. 8, pp. 1–144.
[20] K. De'Bell and T. Lookman, Rev. Mod. Phys. **65**, 87 (1993).
[21] E. Eisenriegler, *Polymers Near Surfaces* (World Scientific, Singapore, 1993).
[22] While our paper deals exclusively with ideal polymers, similar scaling forms (albeit with different exponents) apply to real polymers or SAWs. Indeed, preliminary work indicates striking qualitative (and even quantitative) similarities for SAWs.
[23] J. Cardy, *Scaling and Renormalization in Statistical Physics* (Cambridge University Press, Cambridge, UK, 1996).
[24] J. L. Cardy and S. Redner, J. Phys. A **17**, L933 (1984).
[25] M. N. Barber, A. J. Guttmann, K. M. Middlemiss, G. M. Torrie, and S. G. Whittington, J. Phys. A **11**, 1833 (1978).
[26] D. Sarid, *Scanning Force Microscopy* (Oxford University Press, New York, 1994).
[27] F. J. Giessibl, Rev. Mod. Phys. **75**, 949 (2003).
[28] G. E. Crooks, Phys. Rev. E **60**, 2721 (1999).
[29] D. Collin, F. Ritort, C. Jarzynski, I. Tinoco, Jr., and C. Bustamante, Nature **437**, 231 (2005).
[30] E. Ben-Naim and P. L. Krapivsky, J. Phys. A **43**, 495008 (2010).
[31] E. Ben-Naim, Phys. Rev. E **82**, 061103 (2010).
[32] R. Bubis, Y. Kantor, and M. Kardar, Europhys. Lett. **88**, 48001 (2009).